Physica D 62 (1993) 186–191
North-Holland

PHYSICA D

Poincaré versus Boltzmann in Šil'nikov phenomena

F.T. Arecchi, A. Lapucci and R. Meucci
Istituto Nazionale di Ottica, largo E. Fermi 6, Firenze, Italy

By suitable adjustment of the control parameters in a CO_2 laser with feedback we show experimental evidence of Šil'nikov chaos, characterized by intensity pulses almost equal in shape, but irregularly separated in time. The times of return to a Poincaré section are statistically spread, however their iteration map is one-dimensional and in close agreement with that arising from Šil'nikov theory. Thus, the iteration map of the time intervals becomes the most appropriate indicator of this chaos. The residual width of the experimentally measured maps is due to a transient fluctuation enhancement peculiar to macroscopic systems, which is absent in low-dimensional chaotic dynamics. This appears as an inestricable mixture of deterministic unpredictability as introduced by Poincaré and stochastic fluctuations as considered in Boltzmann statistical mechanics.

By Šil'nikov dynamics we denote a global dynamics in at least a 3D phase space characterized by the presence of orbits asymptotic to an unstable saddle focus [1]. This is a sample of the general class of chaotic behaviors ruled by the presence of one or more unstable attractors and of some asymptotic trajectories connecting their stable and unstable manifolds. In presence of such phase space structures the motion consists in orbits wandering from one attractor to the other (heteroclinic behavior) or looping around one attractor (homoclinic behavior).

The optical implementation of a Šil'nikov dynamics has been shown in lasers with external feedback. The characterization is done in terms of iteration maps of the successive return times to a given Poincaré section. This may be considered as an extension of the Passage Time Method [2] to the case of multiple passages.

Let us consider a dynamics with fixed points all unstable, within a given range of control parameters. We call such situation a regime of competing instabilities [3]. In presence of a saddle focus and limiting our analysis to a 3D space, let us call $\alpha \pm i\omega$ the pair of complex eigenvalues on the stable ($\alpha < 0$) manifold and $\gamma > 0$ the eigenvalue in the unstable direction orthogonal to the stable plane. In our physical implementations [4] we can adjust the control parameter in order to isolate a non zero set of initial conditions such that all trajectories departing from there visit the neighbourhood of the unstable saddle focus and remain at a finite distance from all other fixed points. In such a case, under the Šil'nikov condition

$$|\alpha/\gamma| < 1 \tag{1}$$

the motion becomes chaotic.

Two orbits of this type spiralling around an unstable saddle focus are qualitatively sketched in fig. 1. With the understanding that the only interesting dynamical features occur around the unstable point we obtain a global description by just studying the linearized dynamics within a small box. We orient the three axes along the eigenvectors with x–y coinciding with the stable plane and z being the expanding direction. We take the π plane (vertical plane of equation $x = 1$ containing a face of the cube) as the Poincaré section and we calculate the return map for the coordinate z. Starting at $t = 0$ at $z = 0$ on $x = 1$ (y is irrelevant for the following considerations) the phase point leaves the upper cube side $z = 1$

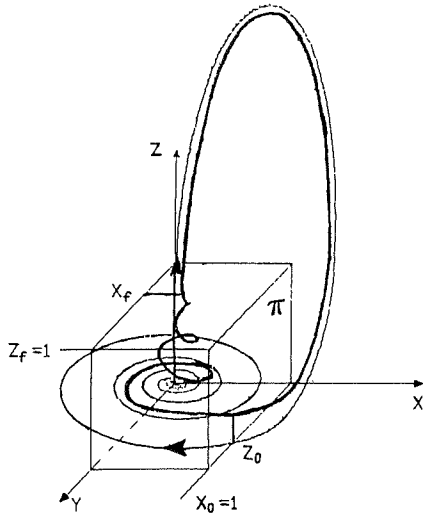

Fig. 1. Schematic rappresentation of a trajectory in Šil'nikov dynamics and construction of unit box leading to the unidimensional map (4) through the linearization of the flow around the saddle focus.

at time τ such that $1 = z_0 e^{\gamma\tau}$, from which results

$$\tau = -\frac{1}{\gamma} \log z_0 . \tag{2}$$

The horizontal coordinate x evolves over the same time as

$$x(\tau) = e^{-\alpha\tau} \cos \gamma\tau , \tag{3}$$

since the initial condition is $x(0) = 1$. Neglecting a phase shift due to the y position, we constrain the motion external to the box to a rigid translation $x(\tau) \rightarrow z_1$ (see dashed trajectories), besides an offset ϵ added at each turn and which may be considered as a second control parameter, the first one being the ratio $|\alpha/\gamma|$. Using relation (2) and writing z as z_{n+1} and z_0 as z_n we obtain the return map

$$z_{n+1} = z_n^{\alpha/\gamma} \cos\left(\frac{\omega}{\gamma} \log z_n\right) + \epsilon , \tag{4}$$

which describes the homoclinic orbits.

The map (4), even though representing a sensible global description, may provide a poor experimental criterion whenever the z coordinates on the π plane are clustered in a small region. A lack of experimental sensitivity appears in experimental return maps which do not display the nice features that eq. (4) provides for the theory. Such was the case for the Belousov–Zabotinsky reaction [5]. On the other hand, the above behavior appears rather universal whenever one can isolate a spiral type orbit, as it occurs in Lorenz or Roessler chaos [6].

In dealing with a quantum optical experiment we introduced a more sensitive dynamical indicator [4]. Based on the logarithmic relation between position z on the π plane and time τ that the orbits take to return to that plane, and assuming that the relevant time is that spent in the box of fig. 1, eq. (4) transforms via relation (2) into a return map for orbital times. Rescaling τ as $T = \gamma\tau = -\log z$ one obtains

$$\begin{aligned} T_{n+1} &= -\ln[\exp(-\alpha/\gamma T_n) \cos(\omega/\gamma) T_n + \epsilon] \\ &= -\ln[\phi(T) + \epsilon] . \end{aligned} \tag{5}$$

Comparison of eqs. (4) and (5) shows the enhanced sensitivity to fluctuations of the T map with respect to the z map. Indeed, suppose that the offset ϵ from homoclinicity is affected by a small amount of noise. The sensitivities of the two maps to such a noise are given, respectively, by $\partial z/\partial\epsilon = 1$ and

$$\partial T/\partial\epsilon = [\phi(T) + \epsilon]^{-1} . \tag{6}$$

This sensitivity factor acts whenever $\phi(T) + \epsilon$ becomes very small. Note that this is not yet deterministic chaos; in fact, large fluctuations can be expected even for a regular dynamics with a fixed point T^*. Note also that it is not associated with the homoclinicity condition $\epsilon = 0$; in fact, for finite ϵ there may be a T^* such that $\phi(T^*) + \epsilon = 0$.

Since a homoclinic orbit is the dynamic counterpart of repeated decays out of an unstable

state, the result is like repositioning the initial condition in an experiment on a single decay [7]. Here the repetition is automatically provided by the contracting motion asymptotic to the stable manifold. As a consequence, superposed upon the deterministic dynamics (either regular or chaotic), the high sensitivity (eq. (6)) may provide a broadening of the T maps not detectable in the z maps whenever noise in the offset ϵ is present.

The same amount of $\delta\epsilon$ in eqs. (4) and (5) leaves the z maps unaltered, while it strongly affects the T maps. Its effect on T maps is shown in fig. 2. If we specialize the map parameters α, γ, ω, and ϵ to a regular orbit (fixed points both in z and T spaces), introduction of $\delta\epsilon$ does not broaden the z point, while the T point broadens. For example, the values $\alpha/\gamma = 0.98$, and $\epsilon = 0.01$ yield one fixed point $T^* = 5.327$, with a sensitivity $\delta T^*/\delta\epsilon = 182$. Note that the noise effect reported here has nothing to do with additive noise effects on return maps [8]. Indeed, the latter effects refer to the scaling behavior near stationary bifurcations, whereas our data refer to transient fluctuation enhancement, and they do not leave a permanent mark (such as an orbital shift or broadening).

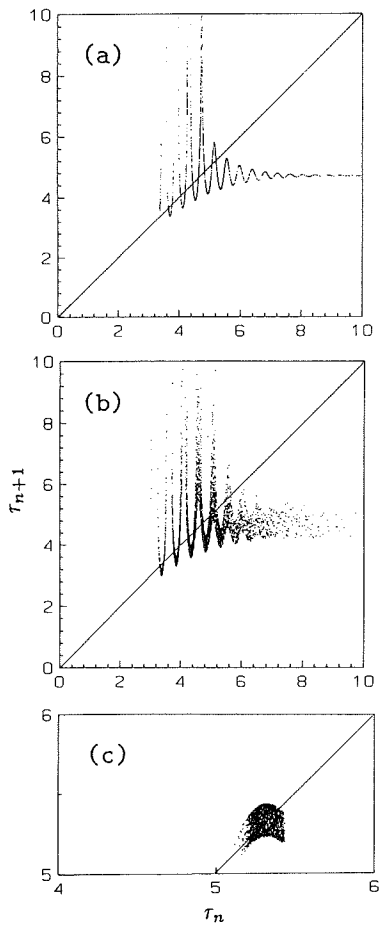

Fig. 2. Numerical iteration maps for return times in Šil'nikov chaos. Parameter values: $\omega/\gamma = 13.0$, $\alpha/\gamma = 0.986$, $\epsilon = 0.01$. (a) and (b) T maps without and with noise $\delta\epsilon = 10^{-2}$, respectively. (c) Stable fixed point of the regular dynamics, broadened by a noise $\delta\epsilon = 10^{-2}$.

In our early experiments on homoclinic chaos [4] such a spread of the return times T gave rise to statistical distributions $P(T)$. Since we had no specific model to fit them, we rather recurred to the iteration maps, as here reported in figs. 2 and 5. A recent numerical experiment on Duffing equation [9] provided a nice fitting of the shape of $P(T)$ with that predicted by a model, however ref. [9] does not discuss the correlation between successive return times as done here.

Thus, while Šil'nikov chaos is a deterministic effect described on average by the backbone of the z or T maps, the superposed thickening is a noise effect peculiar to T maps and undetectable in z maps. This new effect is a specific indicator of intrinsic fluctuations, and it permits a demarcation line to be drawn between a real experiment and a noise free model simulation, from which this second feature is absent.

In fact, the model description $\dot{x} = F(x)$ of a large system in terms of a low-dimensional dynamic variable x is just an ensemble-averaged description, and residual fluctuations on position x must be considered at some initial time, even though the successive evolution is accounted for by a deterministic law. In our case such a fluctuation is a stochastic spread $\delta\epsilon$ on the offset ϵ and it sensitivity thickens the T maps. These considerations show that the system we are exploring cannot be considered on a purely dynamical basis, but, if we take as indicators the T maps, also the statistics of the fluctuations around the

dynamical mean motion must be taken into account.

After having summarized the main features of Šil'nikov chaos we describe the corresponding experiments.

The experimental setup consists of a single mode CO_2 laser with a loss modulator driven by a signal proportional to the laser output intensity. Single mode CO_2 laser dynamics is described by two coupled differential equations, for the laser intensity $x(t)$ and the population inversion $y(t)$. The presence of a feedback signal $z(t)$ introduces a third degree of freedom. Such a system is described by three first-order differential equations for $x(t)$, $y(t)$, and $z(t)$. Keeping all other parameters fixed, the dynamics is controlled by varying a bias voltage B in the feedback loop.

We can visualize $x - z$ phase-space projections, by feeding onto a scope the photodetector signal proportional to the laser output intensity $x(t)$ and the feedback voltage $z(t)$. This phase-space projection consists of closed orbits visiting successively the neighborhoods of the three unstable stationary points 0, 1, and 2.

The local chaos around point 1, established at the end of a subharmonic sequence, has been characterized by standard methods as power spectra and correlation dimension measurements [10]. The competition of the three instabilities in controlling the global features of the motion was described in ref. [3]. Here the control parameters are adjusted in order to have a dominance of the saddle focus, so that the motion consists of a quasi-homoclinic orbit asymptotic to it.

Fig. 3 reports experimental plots of the laser intensity vs. time for two slightly different conditions. Fig. 3b shows evidence of a homoclinic orbit in the two long transients, which provide a lengthy permanence in a phase space region of almost constant intensity. This appears more clearly in the corresponding phase space projections (figs. 4a, 4b). For comparison we give in fig. 4c a photographic exposure (over 1 s) of 30 000 orbits similar to the single one of fig. 4a, to show the stability of shape.

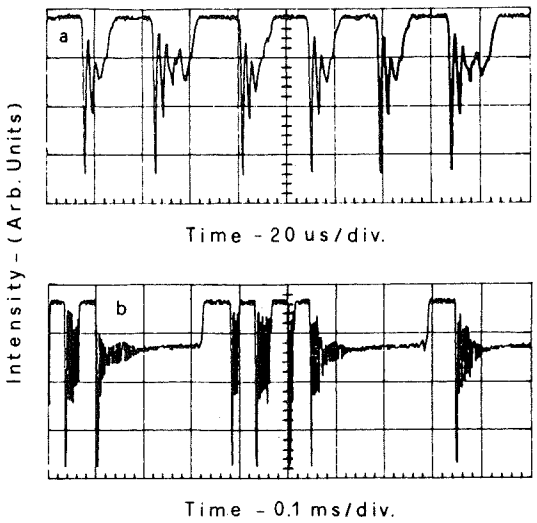

Fig. 3. Time plots of the laser intensity in the regime of Šil'nikov chaos. (a) and (b) refer to two different gains of the feedback loop. (b) shows two long transients corresponding to a large number of small spirals around the saddle focus.

The time spacings are measured by setting a threshold circuit near the top of the largest peak of the intensity signal. An appropriate Poincaré section $x =$ constant can be selected by adjusting the threshold level of a discriminator. A time-to-amplitude converter (TAC) yields the sequence T_i of successive time spacings, which is then classified as a statistical distribution by a multichannel pulse height analyser, or stored in a digitizer, so that correlation functions or iteration maps can be sorted out.

The statistical distribution of return times is a broad featureless curve which does not offer cues on the ordering of T_i. On the contrary, the iteration map (T_{i+1} vs. T_i) displays a regular structure (fig. 5a). To check whether we are in the presence of a one-dimensional (1D) iteration map, and the remaining thickness is due to the observation technique, or the map is more that 1D, we report in fig. 5b the iteration maps corresponding to three regular situations.

In the absence of fluctuations in T_i they should be pointlike (the image of a stable fixed point). In fact spot 1 of fig. 5b is the calibration with an electronic oscillator and it just shows the resolution of the TAC, spot 2 corresponds to the laser

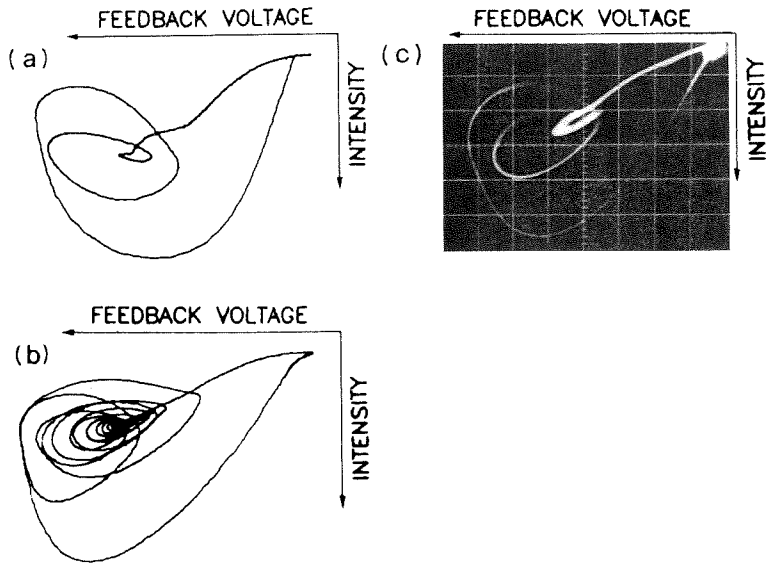

Fig. 4. Phase space projections $x-z$ (laser intensity-feedback voltage). (a) and (b) are single orbits obtained by a digitizer, referring to the same parameters of fig. 3a and 3b, respectively. (c) is the superposition of 30 000 orbits of type (a).

in a regular periodic regime away from the Šil'nikov instability, and spot 3 corresponds to the laser on the verge of the instability but still with a regular period. In this last case, the fluctuation associated with the nearby transition shows that, even without chaos in the return time, the close approach to an instability point introduces a fluctuation enhancement, which has no theoretical counterpart in the current treatment of deterministic chaos. To deal with this broadening, the dynamical equations should include a statistical spread in the injection coordinate at the Poincaré section near the saddle focus, to account for the macroscopic character of the experimental system. As it was shown in ref. [7], even though this spread has no relevance on the average dynamics, it contributes a large transient fluctuation whenever the system decays from an unstable point.

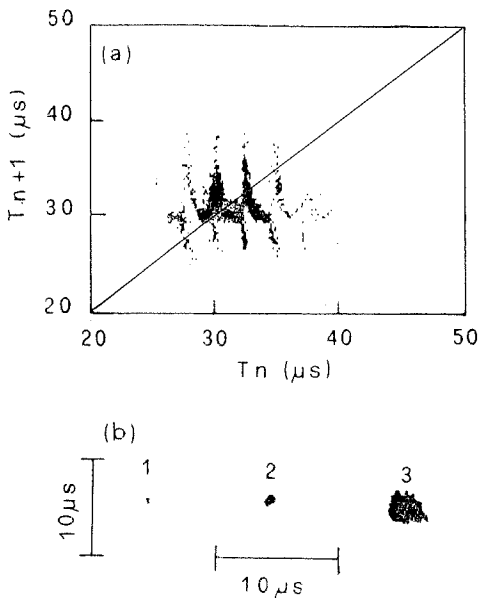

Fig. 5. Experimental iteration maps of the return times. (a) refers to fig. 3a. (b) shows the maps corresponding to regular periodic situations, namely, (1) an electronic oscillator, (2) the laser in a regular periodic regime and (3) the laser just at the onset of the instability but still with a regular period.

This suggests a consideration at the borderline between system dynamics and statistical mechanics. Nonlinear chaotic dynamics is described by a small number of coupled equations

$$\dot{x}_i = F_i(\{x_i\}) , \tag{7}$$

where $\{x_i\} = x_1, x_2, \ldots, x_N$, and $N \geq 3$. In elementary systems as a driven pendulum, x_i are associated with simple variables as momentum, coordinate and driving amplitude of the pendulum. Whenever the system is a macroscopic

one, N is a very large number, and the reduction to a small number of coupled collective variables implies suitable ensemble averages. If however there are sizable transient fluctuations as above described, then the collective equations are

$$\langle \dot{x}_i \rangle = \langle F_i(\{x_i\}) \rangle \,. \tag{8}$$

The general dynamics (8) reduces to a mean-field version such as eq. (7),

$$\langle \dot{x}_i \rangle = F_i(\{\langle x_i \rangle\}) \,, \tag{9}$$

used in models or computer simulations, only whenever

$$\langle \delta x_i^2 \rangle / \langle x_i \rangle^2 \ll 1 \,. \tag{10}$$

This is by no means the case in the Šil'nikov dynamics here described. Indeed, as shown in refs. [7] and [11], transient anomalous fluctuations imply $\langle \delta x_i^2 \rangle / \langle x_i \rangle^2 = \mathcal{O}(1)$. A proper introduction of Langevin forces $\eta_i(t)$ can reduce the complex situation (8) to the simpler functional form (9) for the macroscopic variables $X_i \equiv \langle x_i \rangle$, that is,

$$\dot{X}_i = F_i(\{X_i\}) + \eta_i(t) \,. \tag{11}$$

In eq. (11), $i = 1, 2, \ldots, M$, where M is a small number (less than 10) and η_i accounts for the other $N - M$ degrees of freedom. Without η, eq. (11) would provide the mean field dynamics which may show the dynamic instabilities studied after Poincaré. For a linear F_i, eq. (11) provides a description of the standard Brownian motion which is the program of Boltzmann's statistical mechanics. Thus far, the two problems, that is, the nonlinear dynamics of small number of degrees of freedom and the statistical mechanics of a small system coupled to a large one which acts as a thermal bath, have been considered as separate scientific endeavours. The experimental system here considered is representative of a class of problems which ask for both treatments in an inestricable way. A full characterization of the Langevin forces $\eta_i(t)$ appears strongly model dependent. While their Gaussian character may be based on general considerations, whether their correlations are short or not (white or colored noise) may depend on a complex intertwinning of dynamical and statistical characteristics. Thus the transient fluctuation enhancements associated with escapes from unstable points have to be dealt with by a wise combination of Poincaré and Boltzmann strategies.

References

[1] L.P. Šil'nikov, Dokl. Akad. Nauk SSSR 160 (1965) 558; L.P. Šil'nikov, Mat. Sb. 77 (1968) 119, 461; 81 (1979) 92, 123;
A. Arneodo, P.H. Coullet, E.A. Spiegel and C. Tresser, Physica D 14 (1985) 327.

[2] F.T. Arecchi and A. Politi, Phys. Rev. Lett. 45 (1990) 1219.
F.T. Arecchi, A. Politi and L. Ulivi, Nuovo Cimento 71B (1982) 119.

[3] F.T. Arecchi, R. Meucci and W. Gadomski, Phys. Rev. Lett. 58 (1987) 2205.

[4] (a) F.T. Arecchi, A. Lapucci, R. Meucci, J.A. Roversi and P. Coullet, Europhys. Lett. 6 (1988) 677;
(b) F.T. Arecchi, W. Gadomski, A. Lapucci, R. Meucci, H. Mancini and J.A. Roversi, J. Opt. Soc. Am. B5 (1988) 1153.

[5] F. Argoul, A. Arneodo and P. Richetti, Phys. Lett. A 120 (1987) 269.

[6] P. Glendinning and C. Sparrow, J. Stat. Phys. 35 (1984) 645;
P. Gaspard, R. Kapral and G. Nicolis, J. Stat. Phys. 35 (1984) 697.

[7] F.T. Arecchi, V. Degiorgio and B. Querzola, Phys. Rev. Lett. 19 (1967) 1168;
F.T. Arecchi and V. Degiorgio, Phys. Rev. A 3 (1971) 1108.

[8] J.P. Crutchfield, D. Farmer and B.A. Hubermann, Phys. Rep. 92 (1982) 45.

[9] E. Stone and P. Holmes, Phys. Lett. A 155 (1991) 29.

[10] F.T. Arecchi, W. Gadomski and R. Meucci, Phys. Rev. A 34 (1986) 1617.

[11] F. Haake, Phys. Rev. Lett. 41 (1978) 1685.